Kondo conductance in an atomic nanocontact from first principles

Kondo Conductance in an Atomic Nanocontact from First Principles

Procolo Lucignano[1,2], Riccardo Mazzarello[1,3,4], Alexander Smogunov[1,3,5], Michele Fabrizio[1,3,6] & Erio Tosatti[1,3,6]

[1]*SISSA, Via Beirut 2/4, Trieste 34014, Italy,*

[2]*Coherentia CNR-INFM, Monte S.Angelo via Cintia, 80126 Napoli, Italy,*

[3]*INFM, Democritos Unitá di Trieste, Via Beirut 2/4, Trieste 34014, Italy,*

[4]*Computational Science, Department of Chemistry and Applied Biosciences, ETH Zurich, USI Campus, Via Giuseppe Buffi 13, CH-6900 Lugano, Switzerland,*

[5]*Voronezh State University, University Square 1, Voronezh 394006, Russia,*

[6]*ICTP, Strada Costiera 11, Trieste 34014, Italy.*

The electrical conductance of atomic metal contacts represents a powerful tool to detect nanomagnetism. Conductance reflects magnetism through anomalies at zero bias[1–7] – generally with Fano lineshapes – due to the Kondo screening of the magnetic impurity bridging the contact.[8,9] A full atomic-level understanding of this nutshell many-body system is of the greatest importance, especially in view of our increasing need to control nanocurrents by means of magnetism. Disappointingly, zero bias conductance anomalies are not presently calculable from atomistic scratch. In this Letter we demonstrate a working route connecting approximately but quantitatively density functional theory (DFT) and numerical renormalization group (NRG) approaches and leading to a first-principles conductance calculation

for a nanocontact, exemplified by a Ni impurity in a Au nanowire. A Fano-like conductance lineshape is obtained microscopically, and shown to be controlled by the impurity s-level position. We also find a relationship between conductance anomaly and geometry, and uncover the possibility of opposite antiferromagnetic and ferromagnetic Kondo screening – the latter exhibiting a totally different and unexplored zero bias anomaly. The present matching method between DFT and NRG should permit the quantitative understanding and exploration of this larger variety of Kondo phenomena at more general magnetic nanocontacts.

The electrical conductance of metals through magnetic nano-contacts, including STM tip tunnelling[1–6] and mechanical break junctions (BJ)[7] displays, in analogy to quantum dots[10], a zero-bias anomaly reflecting a Kondo many body effect.[8,9] First principles calculations of the contact conductance and of the anomalies are currently unavailable. The standard DFT based Landauer method[11] is mean-field in character, and thus invalid in presence of many body effects. Alternatively, the NRG[12] solution of Anderson impurity models (AIM)[13,14] is known to yield correctly the zero-bias conductance[15]: but the AIMs are treated as barely more than toy models, their parameters generally guessed or fixed phenomenologically, rather than based on first principles.

Our approach starts from a first-principles DFT calculation but, instead of ending as usual with the standard calculation of the mean-field conductance[16,17], it continues with the building of geometry-dependent AIMs, each explicitly including the channels, orbitals, and especially symmetries suggested by the DFT electronic structure. The key point is that the numerical parameters are fine tuned by requiring these AIMs to yield in mean field the same phase shifts suffered in

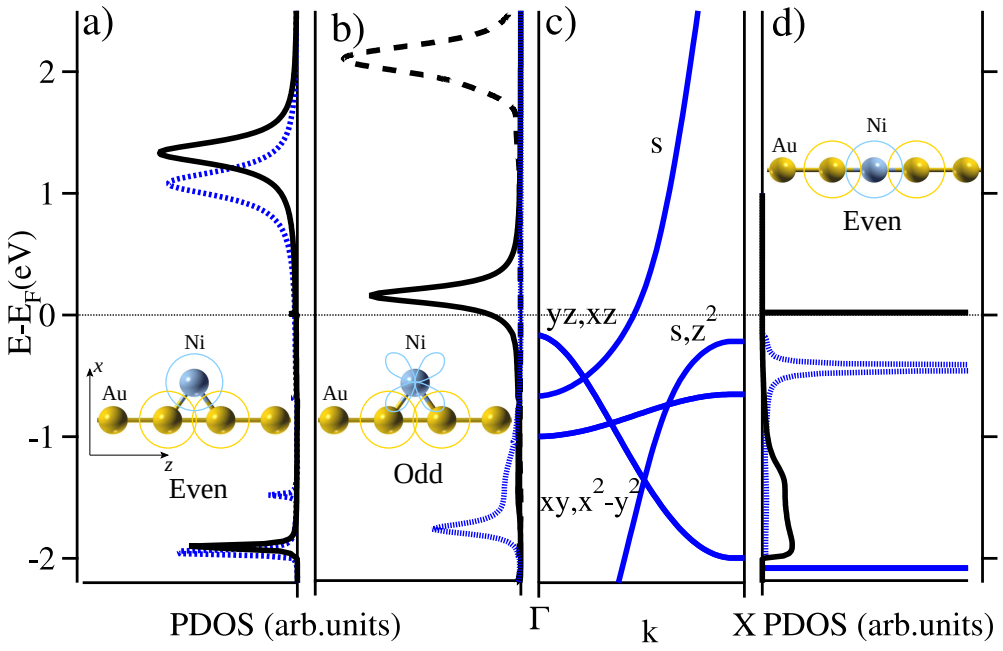

Figure 1: Electronic structure of a Au wire with a Ni impurity in bridge and substitutional geometries. a) DFT projected density of states (PDOS) at the Ni s orbital in bridge geometry. Blue dotted line: spin up; full black line: spin down. b) PDOS at the Ni d_{zx} orbital in bridge geometry. Black dashed line: LDA+U down spin PDOS with $U = 3eV$; c) electronic bands of a clean Au chain; d) PDOS at the Ni d_{zx}, d_{zy} orbitals in substitutional geometry. The effect of U is negligible in this case.

DFT by a spin polarized traveling electron of each symmetry. We exemplify directly our method by straightforward application to a prototype Au-Ni-Au monatomic chain contact, a test system chosen because of its simplicity: in fact, Au possesses just one s-like conduction band, and the Ni bridging impurity is free of complications involving anisotropy and spin-orbit coupling, which affect other transition metal atoms.[4]

We start off from the recent DFT calculation of the nanocontact electronic structure[17] and examine the symmetry-selected projected density of electron states (PDOS). The Ni atom in the Au chain (axis parallel to z) has two low energy geometries: bridge (B) and substitutional (SUB) (left and right insets in Fig. 1). In B (preferred at zero stress) the PDOS indicates a well defined Ni $3d_{zx}$ spin down empty orbital (Fig.1b). The Au chain conduction channel is a single $6s$ nondegenerate band crossing the Fermi energy E_F (Fig. 1c), hybridized with both Ni $4s$ and Ni $3d_{zx}$ orbitals – the first even under reflection across the Ni xy plane, the other odd. Electrons traveling in the Au "leads" will thus scatter differently off the Ni impurity in the two symmetry channels, even (e) and odd (o). The DFT calculated magnetic moment $M = 2\mu_B\langle S_z\rangle$ is $1.30\mu_B$, enhanced over the bare value of a $S = 1/2$ impurity state by co-polarization of nearby Au atoms, but dropping in fact to $\sim 1.0\mu_B$ after correction of DFT through a Hubbard-U term (so-called LDA+U) which raises the $3d_{zx}$ energy[17] (dashed curve in Fig.1b). Summing up, the B geometry implies electron hopping across Ni $3d_{zx}$ which has odd symmetry and $S \sim 1/2$, as well as across Ni $4s$ which has even symmetry and is very little spin polarized. In SUB geometry (of higher total energy[17], but probably accessible at large stress), the electron states can be labeled by m, the orbital angular momentum about the z axis. The empty spin-down Ni state orbitals are now a $3(d_{zx}, d_{zy})$ degenerate pair with

$|m| = 1$. Orthogonality to the $m = 0$ Au conduction band results in a PDOS δ-like peak just 0.02 eV above E_F (Fig. 1d). This suggests $S = 1$; and the DFT calculated Ni magnetic moment is in fact $M = 1.91\mu_B$, rising to $2.02\mu_B$ upon addition of a U term.[17] Summing up, in the SUB geometry the Ni impurity has $S \simeq 1$ and the magnetic orbitals are "spectators". The Au conduction electrons hop onto the Ni $4s$ orbital in the even symmetry channel, whereas they find no Ni valence orbital in the odd channel.

The DFT calculations also provide the electron transmission matrix through the impurity, yielding directly the Landauer ballistic conductance. However, in standard DFT the moment is artificially frozen, breaking spin rotational invariance, thus wrongly predicting a different conductance for spin up and spin down electrons[17] – in zero external field there simply is no telling what is up and what is down. Through the Kondo effect,[8] symmetry is restored by screening of the spin by the conduction electrons. This many body effect is usually studied by applying a viable spin-symmetric technique such as the NRG[12] to a microscopic, but phenomenological AIM. This wastes the detailed information provided by DFT, unless some way is found to preserve it. The extraction of Anderson model parameters from DFT has a long history.[18] Very recent work on Fe impurities in bulk Au and Ag also addressed this problem.[19] Our proposed joining step between DFT and NRG is the construction of a different, specifically designed Anderson model for each symmetry and geometry, with parameters embodying quantitatively the DFT calculated electron-impurity scattering amplitudes and phase shifts. For each symmetry (e or o) an incoming electron wave with spin initially along x will, after scattering on Ni (magnetic moment parallel to the z-axis), rotate in the $x - y$ plane, clockwise if the coupling is FM or counter-clockwise if it is AFM. Within DFT,

Angle (rad)	Bridge DFT (HF-AIM)	Subst. DFT (HF-AIM)
θ_e	-0.28 (-0.28)	-0.19 (-0.19)
θ_o	1.10 (1.17)	-0.12 (-0.00)

Table 1: **Deflection angles.** Spin rotation angles $\theta_{e/o}$ (at the Fermi energy) of an incoming transverse-polarized conduction electron wave after scattering at the Ni impurity for even and odd conduction channels. DFT ab initio angles are compared with the AIM Hartree Fock ones (in brackets), optimized by adjusting the AIM parameters. Positive $\theta_{e/o}$ correspond to antiferromagnetic electron-impurity coupling, negative to ferromagnetic. θ_o substitutional is zero in the AIM model, as there is no Ni empty valence orbital of this symmetry, and inter-site exchange is neglected.

electron-impurity scattering leads to calculable spin rotation angles, $\theta_{e/o} = 2(\delta^{\downarrow}_{e/o} - \delta^{\uparrow}_{e/o})$, which measure the phase shifts and thus the coupling sign and strength of the Ni impurity spin to the Au conduction electrons. The DFT calculated rotation angles (Table 1) show that in geometry B the coupling is large and AFM in the odd channel, small and FM in the even channel. In geometry SUB the coupling is on the contrary weakly FM in both channels.

We now have all the ingredients needed to construct the minimal AIMs which describe the Au-Ni-Au contact. The models must include the Ni $4s$ orbital, with energy ϵ_s and creation operator $s^{\dagger}_{\sigma}$, and the $3d_{\alpha}$ orbitals, with energies ϵ_{α} and creation operators $d^{\dagger}_{\alpha\sigma}$, where σ denotes spin and $\alpha = xy, xz, \ldots$ labels orbital symmetry. Electron transport in the Au leads takes place in the $6s$ band (the $5d$ band is filled) leading to Au conduction state combinations with $p = e, o$ spin-σ

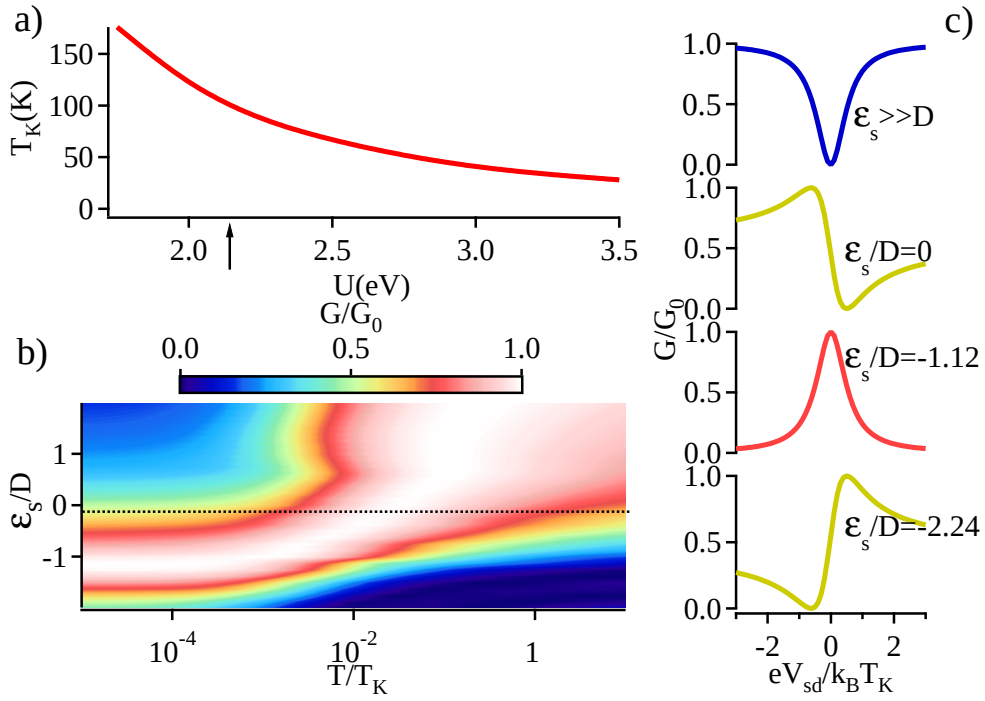

Figure 2: Conductance properties in the bridge geometry. a) NRG calculated Kondo temperature T_K illustratively shown as a function of the on-site d_{zx} interaction U. The physical value for Ni $3d_{zx}$ is indicated by the arrow. b) Color plot of the zero bias conductance as a function of temperature (normalized to the Kondo temperature) and of the effective s orbital energy ϵ_s/D treated as a parameter for illustrative purposes. The physical value for Ni $4s$ is indicated by the horizontal line. When $\epsilon_s >> E_F$ the low temperature ($T < T_K$) conductance is zero, and increases by moving ϵ_s towards E_F, hitting a maximum at $\epsilon_s \sim -D$, declining below -D. c) Low temperature differential conductance as a function of bias voltage V_{sd} applied to the junction. The color of curves refer to the value of ϵ_s in the left bottom panel. Note the Fano lineshapes, due to variation of the even-odd channel interference with varying ϵ_s. (See supplementary material).

creation operators $c^{\dagger}_{\mathbf{k}p\sigma}$ and energy $\epsilon_{p\mathbf{k}}$. The AIM Hamiltonians have the general form

$$\begin{aligned} H &= \sum_{\mathbf{k}p\sigma} \epsilon_{p\mathbf{k}}\, c^{\dagger}_{\mathbf{k}p\sigma} c_{\mathbf{k}p\sigma} + \sum_{\mathbf{k}\sigma} V_{\mathbf{k}s} \left(c^{\dagger}_{\mathbf{k}e\sigma} s_{\sigma} + H.c. \right) \\ &+ \sum_{\mathbf{k}p\sigma} \sum_{\alpha} V_{\mathbf{k}p\alpha} \left(c^{\dagger}_{\mathbf{k}p\sigma} d_{\alpha\sigma} + H.c. \right) \\ &+ \sum_{\sigma} \epsilon_s\, s^{\dagger}_{\sigma} s_{\sigma} + \sum_{\sigma\alpha} \epsilon_{\alpha}\, d^{\dagger}_{\alpha\sigma} d_{\alpha\sigma} + H_{int}\left[s, d_{\alpha}\right]. \end{aligned} \tag{1}$$

In (1), $V_{\mathbf{k}s}$ and $V_{\mathbf{k}p\alpha}$ are hybridization parameters between leads and impurity orbitals, while $H_{int}\left[s, d_{\alpha}\right]$ includes the mutual interactions between impurity orbitals. All parameters in (1) depend on the geometry of the contact, and must reflect the physics provided by the DFT calculation. Our practical procedure is to estimate first approximate AIM parameters from direct inspection of the DFT electronic structure PDOS, and to operate successively a finer adjustment by comparison of the Hartree-Fock calculated AIM spin rotation angles with those directly provided by DFT. Because the AIMs include only a few orbitals and interactions, the agreement is semi-quantitative: yet it can, as we will show, be made very significant.

Bridge – In B geometry, the Ni $3d_{zx}$ orbital is directly hybridized with the odd conduction states, the Ni $4s$ with the even states, and all other Ni $3d$ states can be dropped. The interaction H_{int} includes a Hubbard $U \sim 2\mathrm{eV}$ (deduced by the exchange splitting of spin minority and majority $3d_{zx}$ PDOS peaks), and an intra-atomic s-d FM exchange $J_H \sim -0.3eV$ (extracted by the spin splitting of Ni $4s$, co-polarized by the magnetic $3d_{xz}$). A band-impurity hybridization width $\Gamma_{zx} = 2\pi\rho_0 V^2_{xz} \simeq 0.25\ eV$ ($\rho_0 \sim 0.1eV^{-1}$ is the conduction band density of states at E_F) is deduced from the broadening of the DFT calculated PDOS Ni $3d_{zx}$ peaks (see Fig.1b). Moreover, the majority and minority peak asymmetry around E_F is strongly reduced by addition of a realistic Hubbard U

in LDA+U (see dashed peak in Fig.1b), so we may assume a particle-hole symmetric $\epsilon_{zx} = -U/2$, with $U \sim 2-3$ eV. Finally, Ni $4s$ is a broader orbital, for which $U \sim 0$ and $\Gamma_s \sim 3$ eV, as extracted from the PDOS linewidth. The s-level energy parameter ϵ_s is at the outset totally uncertain. The fine adjustment to reproduce the DFT spin rotation angle yields $\epsilon_s = -0.4\ eV$, just below E_F. For the sake of illustration, since ϵ_s will sensitively control the Fano lineshape of the conductance anomaly, we choose nevertheless to explore different values of ϵ_s, both above and below E_F, as might be relevant in other nanocontacts. Note that the bridge configuration has an additional direct Au-Au hopping bypassing the impurity (see inset of Fig1b), its effect taken equal to Γ_s (for further detail see supplementary).

The AIM Hamiltonian (1) with the parameters adjusted as above yields in the HF approximation spin rotation angles quite close to those calculated by fully realistic DFT (Table 1, see also supplementary material), so that the low energy description of the B configuration is close to being quantitatively correct. The next step is the NRG treatment of model (1) (see Methods). At low temperatures, J_H becomes irrelevant and the e and o channels behave independently. The conductance $G = G_0 \sin(\delta_e - \delta_o)^2$, where $G_0 = 2e^2/h$, is calculated by following, during the NRG flow, the phase shifts $\delta_{e/o}$ (see Methods). The competition between the Kondo effect in the strongly AFM odd channel and the resonance in the weakly FM even channel results in the zero bias conductance plotted in Fig. 2b as a function of temperature and of ϵ_s, the conventional position of Ni $4s$ relative to E_F. At large unphysical $\epsilon_s >> D$ ($D = 2.5eV$ is half bandwidth), both channels acquire a $\pi/2$ phase shift, with a destructive interference and zero conductance. At the fitted value of $-D \ll \epsilon_s < 0$, the conductance is instead expected to be $G/G_0 \sim 0.5$. This deviates

considerably from the DFT calculated Landauer conductance, relatively close to the unitary limit in both spin channels, $G = G_{up} + G_{down} \sim 0.5 + 0.4 \sim 0.9G_0$.[17] The large difference underscores, as anticipated, the impact of Kondo correlations, ignored by DFT. By further decreasing $\epsilon_s < 0$, the conductance reaches its maximum value $G/G_0 = 1$ and then drops. This effect of ϵ_s can be assimilated to that of a gate voltage, controlling the conductance lineshape versus source-drain voltage. Following Ref. 15 we calculated the nonequilibrium conductance as a function of the source-drain voltage V_{sd} (details given in supplementary material). The conductance shows a Fano-like resonance near zero bias, as shown in Fig. 2c, and as expected on general grounds.[9] The large predicted Kondo temperature $\sim 100\ K$, see Fig. 2a, should make this anomaly readily accessible in a break-junction transport experiment.

Substitutional – In SUB geometry, magnetism occurs in $3d_{zx}$ and $3d_{zy}$ Ni orbitals that do not hybridize with the Au $6s$ conduction band. The interaction term $H_{int}\left[s, d_\alpha\right]$ in Eq. (1) should now include all multiplet exchange splittings between $3d_{zx}$ and $3d_{zy}$ degenerate magnetic orbitals. The intra-atomic ferromagnetic exchange with the $4s$ Ni orbital is weak, see the small DFT rotation angles in Tab.1, and all the electron-impurity phase shifts are now FM. Unlike regular AFM Kondo, the ferromagnetic Kondo exchange is well known to be irrelevant at low temperatures, [8] where the magnetic orbitals asymptotically decouple from the conduction band. Only Au $6s$ and Ni $4s$ hybridization will effectively survive, leading to a $\pi/2$ phase shift in the even channel. The zero bias conductance will thus approach unitarity $G(V = 0) \leq G_0$, with a broad Breit-Wigner lineshape of width Γ_s expected for the spectral function. While confirming that, the explicit NRG calculation with the Anderson model (1) with orbitals and parameters appropriate to the SUB

geometry shows in addition that the FM Kondo antiscreening mechanism gives rise at the Fermi level to a logarithmically sharp spectral function"pimple", see Fig. 3 (right panel) and also Ref. 20, pushing G/G_0 up to unity at zero bias. This is again different from the DFT Landauer mean field conductance,[17] $G_\uparrow + G_\downarrow \sim (0.40 + 0.38)G_0 \sim 0.8G_0$. The lineshape difference of this expected "ferro Kondo" anomaly in SUB geometry and of the Fano lineshape of ordinary Kondo in B geometry, respectively right and left panels in Fig. 3, is striking. More generally, no ferro Kondo zero bias anomaly appears to have been reported so far anywhere, so its existence in the present or in other nanocontacts is open for experimental detection. While more work will be needed to describe the effect of a magnetic field in a ferro Kondo case, the effect of temperature should be to cut off the logarithmic cusp, modifying the conductance in the form $1 - const/\ln^2 T$. The final conceptual aspect of spin rotational symmetry is worth mentioning. As is well known,[21] in the regular AFM Kondo, for example of our B geometry, the impurity approximate $S = 1/2$ is absorbed by Kondo screening into an exact singlet, a trivially rotationally symmetric state. In the FM Kondo coupling of SUB geometry the impurity's approximate $S = 1$ is turned by Kondo *antiscreening* into an exact triplet, fully SU(2) rotationally symmetric, endowed with its $2S + 1$ degeneracy.

Summarizing, this work represents a first attempt at joining together the quantitative advantages of DFT electronic structure with the correct NRG many body Kondo physics of a magnetic impurity in a break junction metal contact. Because the intermediate Anderson models can only represent approximately the full electronic processes, the procedure is semi-quantitative. It is nonetheless revealing, showing in the regular Kondo case an *ab initio* example of Fano lineshape;

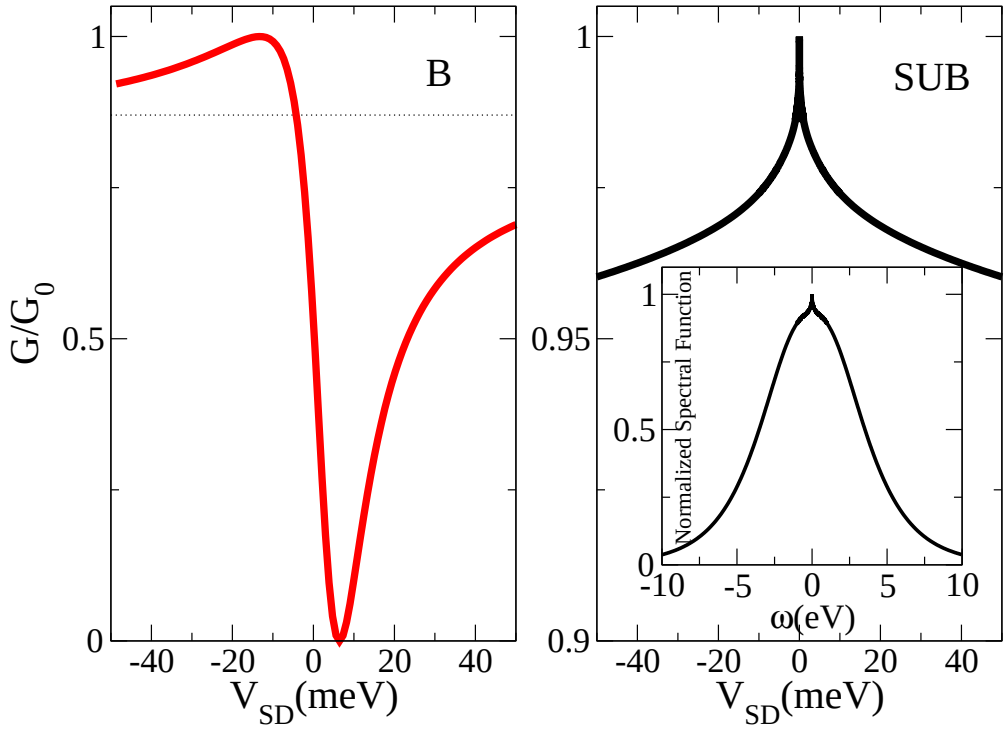

Figure 3: Conductance vs. source-drain voltage of regular and of Ferro Kondo in the two geometries. Sketch of the different zero bias anomalies expected for the current through an Au-Ni-Au junction in the B (left panel), with realistic $\epsilon_s = -0.4$ eV, and SUB (right panel) geometry. Opposite to the Fano lineshape calculated in the B geometry (see also Fig.2c), the Kondo antiscreening in SUB geometry yields a spectral function (see inset) which, for small energies, exhibits a logarithmic "pimple" (see text).

involving phase shifts and Kondo processes that are sometimes ferromagnetic and involve antiscreening; and predicting very different zero bias anomalies depending on impurity geometry and spin. The method should be applicable more generally, whenever well defined intermediate AIMs a) can be built and b) are soluble. On the experimental side, numerous magnetic atom nanocontacts have been realized using STM[3–6]. Mechanical break-junction studies have just begun, so far exploring a different type of phenomenon, namely the emergence of Kondo effects in ferromagnetic metals[7], but many more should be possible in the future, when the kind of antiferro-ferro Kondo switching described here should hopefully be pursued.

METHODS

DFT We carried out DFT calculations within the spin-polarized generalized-gradient approximation (σ-GGA) with the Perdew-Burke-Ernzerhof parametrization [22] for the exchange and correlation energy, with same parameters as in Ref.17. All the calculations were done with the plane wave `PWscf` code, included in the `QUANTUM-Espresso` package. [23] Ultrasoft pseudopotentials [24] were employed and kinetic energy cutoffs of 30 Ry and 300 Ry were used for the wave functions and the charge density, respectively. For both B and SUB geometries, the Au-Au bond length was taken 2.80 Åto avoid spurious magnetizations due to DFT self-interaction errors, [17] whereas all the Au-Ni distances were fully optimized. The calculation supercell consisted of 16 Au atoms plus one Ni atom periodically repeated in all three directions. The wire-wire distance in the xy plane (perpendicular to the wire axis z) was 10.58 Å, making spurious interactions between periodic replicas negligible. In the B configuration, the Ni atom lies in the xz plane. Convergence with respect to k-points and smearing parameters was carefully checked.

Transmission and reflection amplitudes, and the spin rotation angles (see the Supplementary material) were calculated using the Choi and Ihm's method [11] generalized to ultrasoft pseudopotentials, [25] as implemented in the PWCOND code (a part of the `QUANTUM-Espresso` package). The self-consistent potential in the first part of the supercell described above, of length equal to the Au-Au distance, was used to build the periodic potential of the left and right leads, while the potential in the rest of the supercell was used as the scattering region. The zero bias ballistic conductance was obtained using the Landauer-Büttiker formula [26] from the transmission coefficient at

E_F (with all spin moments frozen). Spin-orbit effects were not taken into account in the present study. The PDOS in Fig. 1 were calculated directly from the scattering states.

NRG In our NRG code (for a review see Ref. 12) we implement the $U(1)$ charge symmetry (quantum number Q, the total charge with respect to one electron per site and orbital) and the $SU(2)$ spin symmetry (quantum number S, the total spin). We choose the Wilson discretization parameter $\Lambda = 2$ (or 1.8 when calculating the Green functions), and keep up to 1500 states per iteration when calculating dynamical quantities, or 800 if we are only interested in the energy spectrum. The Kondo temperature can be expressed as[8] $T_K = \frac{\pi w Z \Gamma}{4 k_B}$ where $w = 0.4128$ is the Wilson coefficient, Γ the hybridization linewidth in the magnetic channel, and Z the quasiparticle residue. The latter can be extracted from the self-energy according to: $Z^{-1} = 1 - (\partial \Sigma(i\omega_n)/\partial\, i\omega_n)|_{i\omega_n=0}$. The self-energy is $\Sigma = -G^{-1} + G_0^{-1}$ where G and G_0 are the impurity Green functions calculated by NRG, respectively in the presence and absence of interaction. The resulting Kondo temperature in our model is shown in Fig. 2 as a function of U. In the bridge geometry the zero bias conductance is evaluated as a function of temperature by direct inspection of the NRG flow. It can be expressed as $G = 2e^2 \sin^2(\delta_e - \delta_o)/h$. The phase shift $\delta_{e/o}$ are related to the two lowest energies of states with quantum numbers $(Q, S) = (1, 1/2)$, which correspond to the cost of adding an even or odd electron to the ground state that has quantum numbers $(0, 0)$. We calculated the difference between these phase shifts, hence the zero-bias conductance, as a function of the temperature T extracted from the NRG iterations. We note however that, while we are quite confident about the values at low temperatures, those at high temperatures must be taken with caution, since the spectrum is still far from a Fermi liquid one. In the substitutional geometry we calculate the Ni $4s$ spectral function

following the guidelines of Ref.27.

1. Knorr, N., Schneider, M. A., Diekhöner, L., Wahl, P. & Kern, K. Kondo effect of single Co adatoms on Cu surfaces. *Phys. Rev. Lett.* **88**, 096804 (2002).

2. Zhao, A. *et al.* Controlling the Kondo Effect of an Adsorbed Magnetic Ion Through Its Chemical Bonding. *Science* **309**, 1542–1544 (2005).

3. Neel, N. *et al.* Conductance and Kondo effect in a controlled single-atom contact. *Physical Review Letters* **98**, 016801 (2007).

4. Otte, A. F. *et al.* The role of magnetic anisotropy in the Kondo effect. *Nature Physics* **4**, 847–850 (2008).

5. Vitali, L. *et al.* Kondo effect in single atom contacts: The importance of the atomic geometry. *Phys. Rev. Lett.* **101**, 216802 (2008).

6. Ternes, M., Heinrich, A. & Schneider, W.-D. Spectroscopic manifestations of the Kondo effect on single adatoms. *J. Phys.: Condens. Matter* **21**, 053001 (2009).

7. Reyes-Calvo, M. *et al.* The Kondo effect in ferromagnetic atomic contacts. *Nature* **458**, 1150–1153 (2009).

8. Hewson, A. *The Kondo Problem to Heavy Fermions* (Cambridge University Press, 1993).

9. Újsághy, O., Kroha, J., Szunyogh, L. & Zawadowski, A. Theory of the Fano resonance in the STM tunneling density of states due to a single Kondo impurity. *Phys. Rev. Lett.* **85**, 2557–2560 (2000).

10. Kouwenhoven, L. P. *et al.* Electron transport in quantum dots. In Sohn, L. L., Kouwenhoven, L. P. & Schon, G. (eds.) *Mesoscopic Electron Transport* (Kluwer Dordrecht, 1997).

11. Joon Choi, H. & Ihm, J. Ab initio pseudopotential method for the calculation of conductance in quantum wires. *Phys. Rev. B* **59**, 2267–2275 (1999).

12. Bulla, R., Costi, T. A. & Pruschke, T. Numerical renormalization group method for quantum impurity systems. *Reviews of Modern Physics* **80**, 395–451 (2008).

13. Glazman, L. I. & Raikh, M. E. Resonant Kondo transparency of a barrier with quasilocal impurity states. *JETP Lett.* **47**, 452–455 (1988).

14. Ng, T. K. & Lee, P. A. On-site Coulomb repulsion and resonant tunneling. *Phys. Rev. Lett.* **61**, 1768–1771 (1988).

15. Meir, Y. & Wingreen, N. S. Landauer formula for the current through an interacting electron region. *Phys. Rev. Lett.* **68**, 2512–2515 (1992).

16. Bagrets, A., Papanikolaou, N. & Mertig, I. Conduction eigenchannels of atomic-sized contacts: Ab initio KKR Green's function formalism. *Phys. Rev. B* **75**, 235448 (2007).

17. Miura, Y., Mazzarello, R., Corso, A. D., Smogunov, A. & Tosatti, E. Monatomic Au wire with a magnetic Ni impurity: Electronic structure and ballistic conductance. *Phys. Rev. B* **78**, 205412 (2008).

18. Gunnarsson, O., Andersen, O. K., Jepsen, O. & Zaanen, J. Density-functional calculation of the parameters in the Anderson model: Application to Mn in CdTe. *Phys. Rev. B* **39**, 1708–1722 (1989).

19. Costi, T. A. *et al.* Kondo decoherence: Finding the right spin model for iron impurities in gold and silver. *Physical Review Letters* **102**, 056802 (2009).

20. Koller, W., Hewson, A. C. & Meyer, D. Singular dynamics of underscreened magnetic impurity models. *Phys. Rev. B* **72**, 045117 (2005).

21. Nozières, P. & Blandin, A. Kondo effect in real metals. *J. Phys. (Paris)* **41**, 193–211 (1980).

22. Perdew, J. P., Burke, K. & Ernzerhof, M. Generalized gradient approximation made simple. *Phys. Rev. Lett.* **77**, 3865–3868 (1996).

23. Baroni, S., DalCorso, A., de Gironcoli, S. & Giannozzi, P. http://www.quantum-espresso.org.

24. Vanderbilt, D. Soft self-consistent pseudopotentials in a generalized eigenvalue formalism. *Phys. Rev. B* **41**, 7892–7895 (1990).

25. Smogunov, A., Dal Corso, A. & Tosatti, E. Ballistic conductance of magnetic Co and Ni nanowires with ultrasoft pseudopotentials. *Phys. Rev. B* **70**, 045417 (2004).

26. Datta, S. *Electronic Transport in Mesoscopic Systems* (Cambridge Studies in Semiconductor Physics and Microelectronic Engineering, 1997).

27. Costi, T. A., Hewson, A. C. & Zlatic, V. Transport coefficient of the Anderson model via the numerical renormalization group. *J. Phys. Condens. Matter* **6**, 2519–2558 (1994).

Acknowledgments We would like to thank D. Basko and C. Untiedt for very useful discussions. The work was supported by the Italian Ministry of University and Research, through a PRIN-COFIN award, and by INFM through "Iniziativa Trasversale Calcolo Parallelo". The environment provided by the independent ESF project CNR-FANAS-AFRI was also useful. P.L. acknowledges financial support from EC STREP project MIDAS "Macroscopic Interference Devices for Atomic and Solid State Physics" and CNR-INFM within ESF Eurocores Programme FoNE-Spintra.

Competing Interests The authors declare that they have no competing financial interests.

Correspondence Correspondence to: Erio Tosatti[1,3,6]. Correspondence and requests for materials should be addressed to E.T. (Email: tosatti@sissa.it).

Author Contributions P.L., M.F. and E.T. conceived and elaborated the Kondo aspects, including NRG; R.M. and A.S. worked out the DFT part, from which A.S. extracted the phase shifts. E.T. wrote the paper, with help from all co-authors.